

Effects of CoO doping on sintering and electrical conductivity of $\text{Ce}_{0.8}\text{Gd}_{0.2}\text{O}_{1.9}$ prepared using CeO_2 powder and Gd precipitation

Young-Hoon Kim and Soo-Man Sim*

Department of Materials Engineering, Hongik University, Sejong City 30016, Korea

This paper reports on the preparation of a fully dense Gd-doped CeO_2 (GDC) at low sintering temperature using CeO_2 powder and Gd precipitation in the presence of CoO as a sintering aid. A mixture of CeO_2 powder and Gd precipitates was calcined at 700 °C followed by milling that resulted in the GDC ($\text{Ce}_{0.8}\text{Gd}_{0.2}\text{O}_{1.9}$) powder with an average particle size of 0.46 μm . Sintering of the undoped sample showed a relative density of 99.2% at 1500 °C, whereas the samples doped with 3 mol% and 5 mol% CoO exhibited a significant densification at the lower temperature reaching a relative density of 98.8% at 1200 °C. The electrical conductivities of both doped samples were almost identical but higher than those of the undoped sample at all measuring temperatures.

Key words: GDC, CeO_2 powder, CoO doping, Sintering, Electrical conductivity.

Introduction

Gd-doped CeO_2 (GDC) has received much attention as an intermediate temperature solid oxide fuel cell electrolyte because of its higher electrical conductivity than that of yttria-stabilized zirconia. However, the synthesis of GDC by solid-state reaction requires sintering temperatures exceeding 1500 °C [1]. Many attempts have been made to decrease the sintering temperature with nano-scale GDC powders produced by various chemical methods including oxalate co-precipitation [2], co-precipitation of hydroxides [3], ammonium carbonate co-precipitation [4, 5], combustion of glycine-nitrate [6], etc. Even though the chemically synthesized powders are highly reactive, they still require relatively high sintering temperatures due to particle agglomeration in the calcined powders [7].

Alternatively, a decrease in the sintering temperature can be achieved by the addition of sintering aids such as transition metal oxides of Mn, Co, and Fe [8-13]. Among these oxides, Co oxide is known to be the most promising one since it enables GDC to be densified at temperatures below 1000 °C [9-13]. However, such doping effects were obtained from chemically synthesized or commercial nano-scale powders. Few studies have been attempted on low-temperature sintering of GDC by the addition of sintering aids to submicron-sized powders.

In the present study, $\text{Ce}_{0.8}\text{Gd}_{0.2}\text{O}_{1.9}$ (GDC20) powder was prepared from the slurry of a mixture of commercial submicron-sized CeO_2 powder and Gd

precipitates and the effects of 3 mol% and 5 mol% CoO doping on sintering and electrical conductivity of the GDC20 were investigated.

Experimental Procedure

A slurry was prepared by injecting 0.5M Gd nitrate ($\text{Gd}(\text{NO}_3)_3 \cdot 6\text{H}_2\text{O}$, 99.9%, Sigma-Aldrich) solution into an attrition jar containing CeO_2 powder (99.99%, Kojundo Chem.) and ZrO_2 balls while being stirred at a low speed. The 1M ammonium carbonate ($(\text{NH}_4)_2\text{CO}_3$, Sigma-Aldrich) solution as a precipitant (2.5 times of the moles of Gd) was slowly added to the jar. The jar was rotated at 500 rpm and the milling was continued until complete precipitation. The resulting slurry, a mixture of CeO_2 powder and Gd precipitates, was filtered and subjected to repeated washing with deionized water and ethanol. The mixture was dried at 80 °C for 12 hrs and then calcined at 700 °C for 4 hrs followed by ball-milling for 2 hrs. For CoO doping, the powder was mixed with Co nitrate ($\text{Co}(\text{NO}_3)_2 \cdot 6\text{H}_2\text{O}$, > 98%, Aldrich) in ethanol, ball-milled for 2 hrs, and calcined at 300 °C in air for 4 hrs. The amounts of CoO corresponded to 3 mol% and 5 mol% of the GDC20. The powder was mixed with a binder (0.5 wt% polyvinyl butyral, Aldrich), uniaxially pressed into pellets of 15 mm diameter at 50 MPa, and subsequently isostatically pressed at 200 MPa. The pellets were heated at 600 °C for 2 hrs to remove the binder and sintered at temperatures between 1100 °C and 1500 °C in air for 4 hrs.

For phase analysis, the powders were heated at temperatures between 400 °C and 1000 °C at a heating rate of 5 °C/min in air for 4 hrs and examined by X-ray

*Corresponding author:
Tel : +82-44-860-2518
Fax: +82-44-862-2774
E-mail: smsim@hongik.ac.kr

powder diffraction with CuK_α radiation (M03XHF, Bruker). Particle size distribution was measured with a laser diffraction particle size analyzer (SALD-2001, Shimadzu). The bulk density of the sintered sample was determined by the Archimedes method and relative density was calculated from the bulk density and the theoretical density of GDC20 [14]. The morphology of the powder and microstructures of the sintered samples were observed with a scanning electron microscopy (FE-SEM, FEI). The electrical conductivities of the sintered samples were measured in the temperature range between 500 °C and 900 °C in air according to four-point DC method. The current source (Model 6220, Precision Current Source, Keithley) was used to supply the current and the voltage drop across the probes was measured with a digital multimeter (Model 2182A, Nanovoltmeter, Keithley).

Results and Discussion

Fig. 1 shows XRD patterns of GDC powders calcined at various temperatures for 4 hrs. The as-prepared powder exhibited only CeO_2 diffraction peaks since the Gd precipitates were in the form of amorphous carbonate. The peak intensities remained unchanged up to 400 °C and then significantly increased at temperatures above 700 °C after complete decomposition of the Gd precipitates. Diffraction peaks due to Gd_2O_3 could not be detected because the main Gd_2O_3 peaks overlapped with CeO_2 peaks [15]. However, the diffraction peaks in the powders calcined above 700 °C could be attributed to CeO_2 solid solution due to the high reactivity of the decomposed nano-crystalline Gd_2O_3 particles. It has been known that the ammonium carbonate co-precipitation method has the advantage of forming a solid solution at relatively low calcination temperature [5]. The samples sintered at 1400 °C for 4 hrs and doped with 0 mol%, 3 mol%, and 5 mol% CoO showed the diffraction peaks coinciding with those of

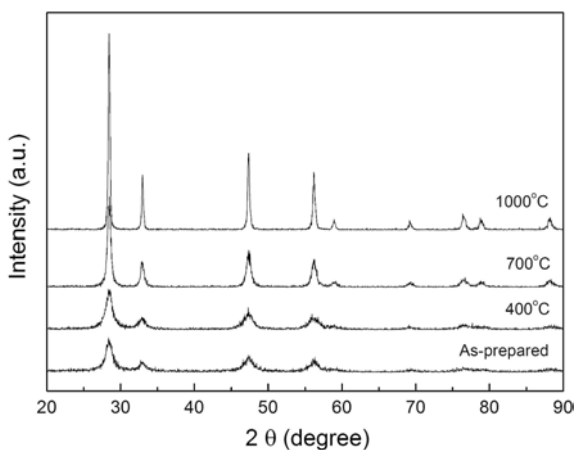


Fig. 1. XRD patterns of GDC powders calcined at various temperatures.

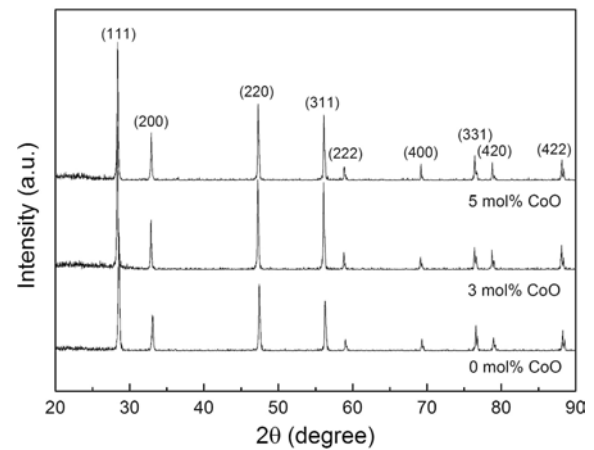


Fig. 2. XRD patterns of GDC samples doped with 0, 3, and 5 mol% CoO and sintered at 1400 °C.

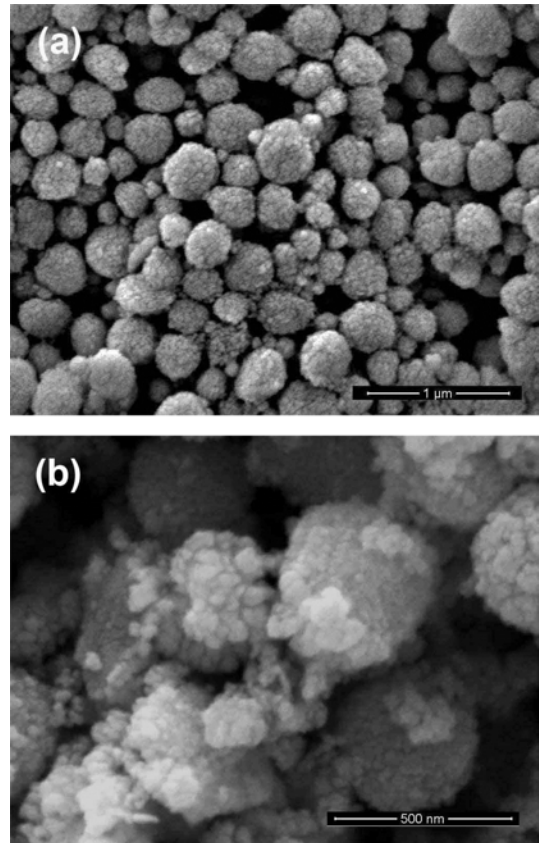


Fig. 3. SEM images of (a) as-received CeO_2 and (b) calcined and milled GDC powders.

GDC20 as indicated by the corresponding Miller indices (Fig. 2) [14]. No diffraction peaks due to CoO were observed in the doped samples.

Fig. 3 shows SEM images of as-received CeO_2 powder and calcined GDC powder. The CeO_2 powder in Fig. 3(a) contained spherical particles consisting of agglomerated primary nanoparticles. The GDC powder in Fig. 3(b) exhibited the same morphology as the CeO_2 powder except that the primary particles grew and

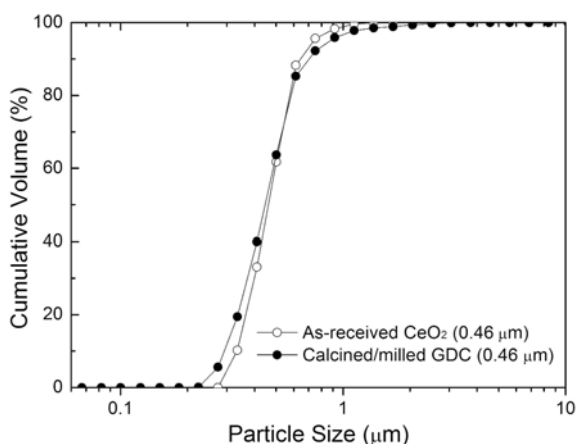


Fig. 4. Particle size distributions of as-received CeO_2 and calcined and milled GDC powders.

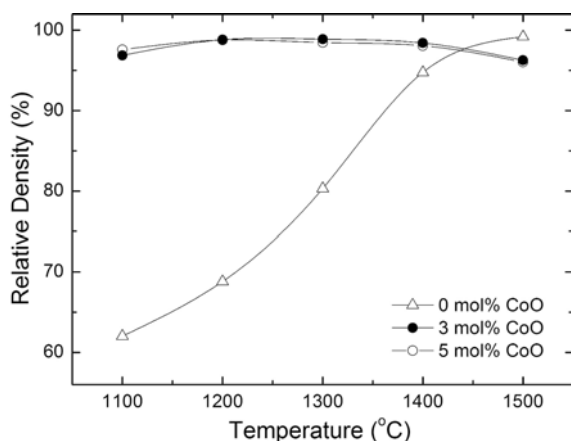


Fig. 5. Relative densities of GDC samples doped with 0 mol%, 3 mol%, and 5 mol% CoO and sintered at various temperatures for 4 hrs

strongly agglomerated in the calcination process. According to the particle size distribution (Fig. 4), the CeO_2 powder had an average particle size of $0.46 \mu m$ and a fairly uniform size distribution ranging from $0.3 \mu m$ to $1 \mu m$. The GDC powder had the same average particle size as that of the CeO_2 powder but a slightly broadened size distribution because of ball-milling.

Fig. 5 represents relative densities of GDC samples sintered at temperatures between $1100^\circ C$ and $1500^\circ C$ for 4 hrs. The undoped sample was barely sintered at $1100^\circ C$ and its density was only 62%. After a gradual increase up to $1400^\circ C$, the density became 99.2% at $1500^\circ C$. CoO doping was found to be effective in lowering the sintering temperature and the doped samples showed the same densification behavior regardless of doping amounts. The samples doped with 3 mol% and 5 mol% CoO were already densified at $1100^\circ C$, resulting in densities of 96.9% and 97.6%, respectively. Their densities reached 98.8% at $1200^\circ C$, which was lower by $300^\circ C$ than the temperature at which the undoped sample had the similar density

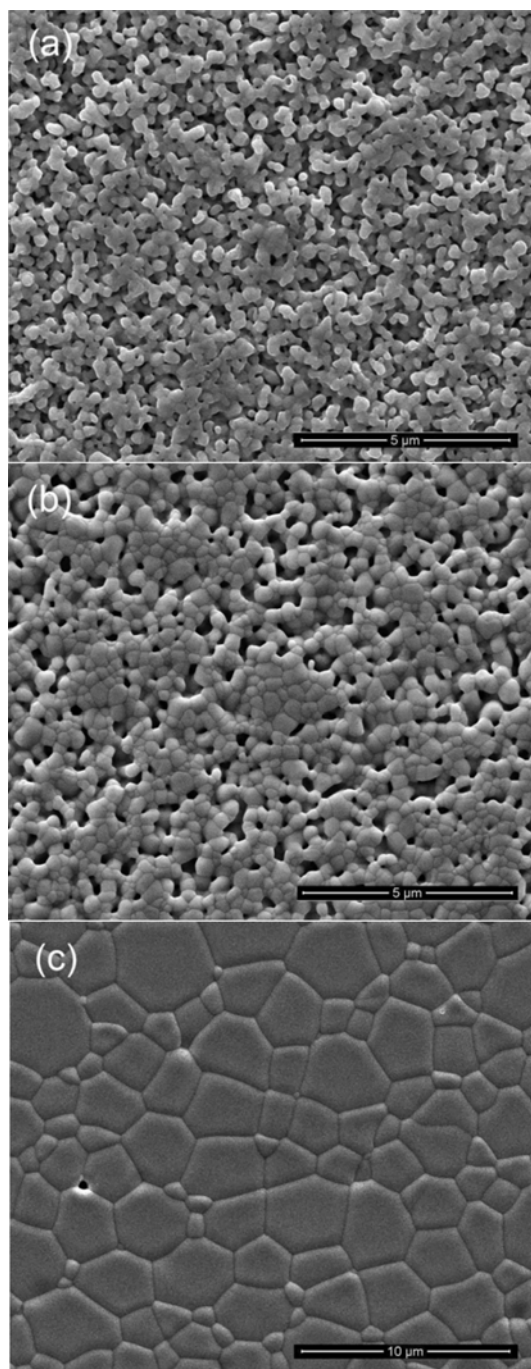


Fig. 6. SEM images of undoped GDC samples sintered at (a) $1200^\circ C$, (b) $1300^\circ C$, and (c) $1500^\circ C$.

(99.2%). However, the densities of the doped samples began to decrease at $1300^\circ C$ and became 96.3% and 96.0% at $1500^\circ C$ for 3 mol% and 5 mol% CoO doping, respectively. The reduction in the densities will be discussed later.

CoO doping in the present study was not effective as much for nano-scale powders, which have better sinterability than submicron-sized powders. Kleinlogel and Gauckler [9] reported a density higher than 99% at $900^\circ C$ by doping GDC20 nano-powder with up to

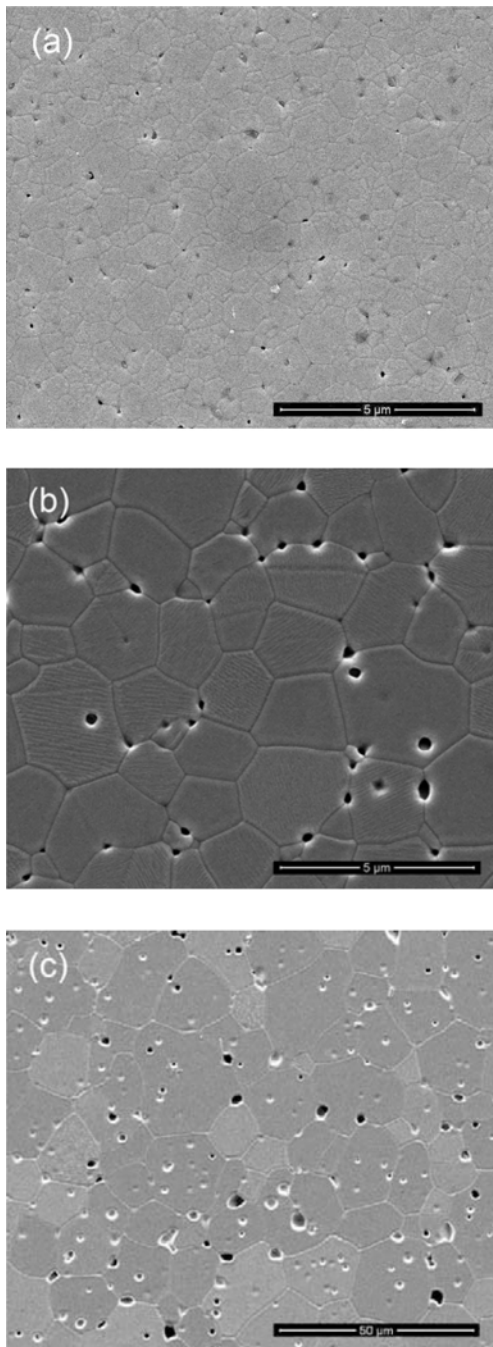


Fig. 7. SEM images of 3 mol% CoO-doped GDC samples sintered at (a) 1200 °C, (b) 1300 °C, and (c) 1500 °C.

5 mol% CoO, while Nicholas and De Jonghe [11] reported densities of 91.6% and 93.3% at 800 °C by doping GDC10 ($\text{Ce}_{0.9}\text{Gd}_{0.1}\text{O}_{1.95}$) nano-powder with 3 mol% and 5 mol% CoO, respectively. Hari Prasad *et al.* [12] claimed to obtain the density of 97% at 850 °C through doping GDC10 powder prepared by co-precipitation of hydroxides with 3 mol% CoO.

Figs. 6(a-c) represent SEM images of undoped GDC sample sintered at 1200 °C, 1300 °C, and 1500 °C, respectively. In Fig. 6(a), the undoped sample sintered at 1200 °C exhibits many pores and necks formed

between particles, indicating the initial stage of sintering. Grains began to form by particle coalescence and pores of irregular shapes were present between particles at 1300 °C (Fig. 6(b)). At 1500 °C, densification was completed, resulting in a fully dense microstructure with well-developed grains of $\sim 5 \mu\text{m}$ in size as shown in Fig. 6(c).

The effect of CoO doping is illustrated in Figs. 7 (a-c) that correspond to SEM images of 3 mol% CoO-doped samples sintered at 1200 °C, 1300 °C, and 1500 °C, respectively. The doped sample sintered at 1200 °C showed a fully dense microstructure with an average grain size of $\sim 1 \mu\text{m}$. However, fine dark gray particles were observed at the grain junctions (Fig. 7(a)). At 1300 °C, the grains grew to $\sim 3 \mu\text{m}$ in size. Concurrently, the dark gray particles disappeared and instead pores appeared (Fig. 7(b)). When the sintering temperature was raised to 1500 °C, these pores became larger and the grains significantly grew to $\sim 20 \mu\text{m}$ in size (Fig. 7(c)). The sample doped with 5 mol% CoO exhibited the same microstructure as the sample doped with 3 mol% CoO at each sintering temperature.

The appearance of the dark gray particles at the grain junctions was attributed to the formation of CoO. The solubility of CoO in GDC was reported to be $< 1 \text{ mol}\%$ at 1100 °C [16]. Jud *et al.* [13] estimated the solubility of CoO to be $< 0.5 \text{ mol}\%$ at 900 °C and found excess CoO in the form of clustering particles at grain junctions. The excess CoO is known to evaporate at 900 °C [16] and the evaporation becomes significant above 1400 °C [17]. Therefore, it is considered that the pores observed at 1300 °C in Fig. 7(b) were produced by the evaporation of CoO, which caused the relative densities to decrease at higher sintering temperatures (Fig. 5).

Fig. 8 shows electrical conductivities of GDC samples as a function of temperature. Undoped and doped samples had densities over 98% after sintering at 1500 °C and 1300 °C, respectively. The doped samples

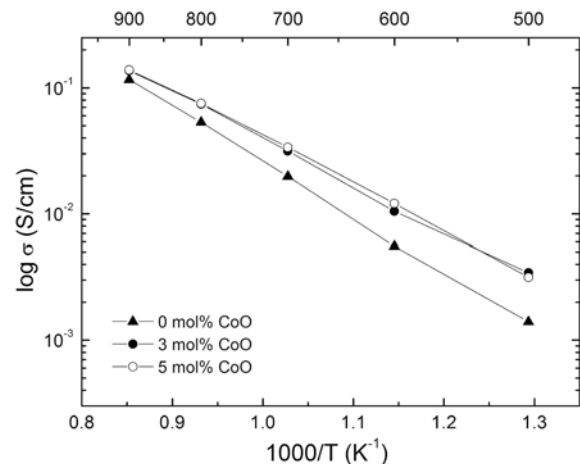


Fig. 8. Electrical conductivities of GDC samples doped with 0 mol%, 3 mol%, and 5 mol% CoO in air.

showed higher conductivities than the undoped sample at all measuring temperatures. The conductivity of the sample doped with 3 mol% of CoO at 600 °C was 1.05×10^{-2} S/cm, which was nearly twofold that of the undoped sample (0.55×10^{-2} S/cm). The sample doped with 5 mol% of CoO showed a slightly higher conductivity (1.21×10^{-2} S/cm).

The effect of CoO doping on the conductivity of GDC exhibits disagreement between literature reports on nano-scale powders [9, 11, 12]. Kleinlogel and Gauckler [9] reported that the conductivity of GDC20 remained unchanged for doping up to 2 mol% CoO (4.8×10^{-2} S/cm at 700 °C) but for doping with 5 mol% CoO sharply decreased compared to undoped GDC. Nicholas and De Jonghe [11] observed the same conductivity of GDC10 doped with up to 5 mol% CoO as that of undoped GDC10. Hari Prasad *et al.* [12] claimed higher conductivity of 3 mol% CoO-doped GDC10 (2.38×10^{-2} S/cm) than that of undoped GDC10 (1.64×10^{-2} S/cm) at 600 °C. The conductivities of the doped GDCs in the present study are not comparable to those reported on nano-scale powders; however, the results demonstrate that low-temperature sintering of GDC derived from submicron-sized CeO_2 powder can be achieved by CoO doping without a loss of conductivity.

Conclusions

$Ce_{0.8}Gd_{0.2}O_{1.9}$ (GDC) powder with an average particle size of 0.46 μ m was prepared through calcination of a mixture of CeO_2 powder and Gd precipitates at 700 °C followed by ball-milling. Sintering of the undoped GDC sample at 1100 °C resulted in a relative density of only 62%, whereas the samples doped with 3 mol% and 5 mol% CoO were densified to relative densities of 96.9% and 97.6%, respectively. The densities of both doped samples became 98.8% at 1200 °C, which was lower by 300 °C than the temperature at which the undoped sample had the similar density (99.2%). The doped samples exhibited higher conductivities than the

undoped sample at all measuring temperatures. The conductivities of the samples doped with 3 mol% and 5 mol% CoO were 1.05×10^{-2} S/cm and 1.21×10^{-2} S/cm at 600 °C, respectively, which were nearly twofold that of the undoped sample (0.55×10^{-2} S/cm).

References

1. H. Inaba and H. Tagawa, *Solid State Ionics* 83 (1996) 1-16.
2. K. Higashi, K. Sonoda, H. Ono, S. Sameshima, and Y. Horata, *J. Mater. Res.* 14 (1999) 957-967.
3. D. Hari Prasad, H.-R. Kim, J.-S. Park, J.-W. Son, B.-K. Kim, H.-W. Lee, and J.-H. Lee, *J. Alloys & Comp.* 495 (2010) 238-241.
4. J.-G. Li, T. Ikegami, Y. Wang, and T. Mori, *J. Am. Ceram. Soc.* 86 (2003) 915-21.
5. A.I.Y. Tok, L.H. Luo, and F.Y.C. Boey, *Mat. Sci. & Eng. A383* (2004) 229-234.
6. L.D. Jadhav, M.G. Chourashiya, K.M. Subhedar, A.K. Tyagi, and J.Y. Patil, *J. Alloys & Comp.* 470 (2009) 383-386.
7. D. Hari Prasad, J.-H. Lee, H.-W. Lee, B.-K. Kim, and J.-S. Park, *J. Ceram. Proc. Res.* 11 (2010) 523-526.
8. R.R. Kondakindia and K. Karan, *Mat. Chem. & Phys.* 115 (2009) 728-734.
9. C.M. Kleinlogel and L.J. Gauckler, *Solid State Ionics* 135 (2000) 567-573.
10. G.S. Lewis, A. Atkinson, B.C.H. Steele, and J. Drennan, *State Ionics*, 152-153 (2002) 567-573.
11. J.D. Nicholas and L.C. De Jonghe, *Solid State Ionics* 178 (2007) 1187-1194.
12. D. Hari Prasad, S.Y. Park, H. Ji, H.-R. Kim, J.-W. Son, B.-K. Kim, H.-W. Lee, and J.-H. Lee, *Ceram. Int.* 38S (2012) S497-S500.
13. E. Jud, Z. Zhang, W. Sigle, and L.J. Gauckler, *J. Electroceram.* 16 (2006) 191-197.
14. Powder Diffraction File, Joint Committee on Powder Diffraction Standards, ASTM, Philadelphia, 1996, Card No. 75-0162.
15. Powder Diffraction File, Joint Committee on Powder Diffraction Standards, ASTM, Philadelphia, 1996, Card Nos. 34-394 and 12-797.
16. M. Mori, Z. Wang, and T. Itoh, *J. Fuel Cell Sci. and Tech.* 8 (2011) 011007-1-6.
17. J.D. Sirman, D. Waller, and J.A. Kilner, *Electrochem. Soc.* (1997) 1159-1168.